Identification of Two Proteins Associated with Mammalian ATP Synthase*[S]

Björn Meyer‡§, Ilka Wittig§, Elisabeth Trifilieff¶, Michael Karas‡, and Hermann Schägger§‖

Bovine mitochondrial ATP synthase commonly is isolated as a monomeric complex that contains 16 protein subunits and the natural IF_1 inhibitor protein in substoichiometric amounts. Alternatively ATP synthase can be isolated in dimeric and higher oligomeric states using digitonin for membrane solubilization and blue native or clear native electrophoresis for separation of the native mitochondrial complexes. Using blue native electrophoresis we could identify two ATP synthase-associated membrane proteins with masses smaller than 7 kDa and isoelectric points close to 10 that previously had been removed during purification. We show that in the mitochondrial membrane both proteins are almost quantitatively bound to ATP synthase. Both proteins had been identified earlier in a different context, but their association with ATP synthase was unknown. The first one had been named 6.8-kDa mitochondrial proteolipid because it can be isolated by chloroform/methanol extraction from mitochondrial membranes. The second one had been denoted as diabetes-associated protein in insulin-sensitive tissue (DAPIT), which may provide a clue for further functional and clinical investigations. ***Molecular & Cellular Proteomics 6:1690–1699, 2007.***

Mammalian mitochondrial ATP synthase, also named F_1F_0-ATP synthase or complex V, uses the electrochemical potential across the mitochondrial inner membrane that is generated by the three major respiratory complexes, NADH dehydrogenase (complex I),[1] cytochrome *c* reductase (complex III), and cytochrome *c* oxidase (complex IV), to synthesize ATP. Other $FADH_2$-linked complexes like succinate dehydrogenase (complex II) do not immediately couple the oxidation of substrates to vectorial proton transport (1–4). F_1F_0-ATP synthase contains an extramembranous F_1- and an intramembranous F_0-domain that are linked by a peripheral and a central stalk (5–8). The central stalk, containing F_1-subunits γ, δ, and ε in mammals, is associated with a ring of F_0-subunits c (9). This central stalk/subunit c assembly constitutes the rotor in the fully assembled ATP synthase. Proton-powered rotation of the c-ring makes the central stalk turn with it, generating torque and conformational changes in the catalytic $\alpha_3\beta_3$ domain of F_1 to synthesize ATP (10–13). Holo-ATP synthase from bovine mitochondria when isolated in monomeric state contains a total of 16 protein subunits (14). Natural inhibitor protein IF_1 is also bound but with variable stoichiometry (15–18).

More recently, mammalian ATP synthase has been isolated also in dimeric and higher oligomeric states using digitonin for membrane solubilization and blue native electrophoresis (BNE) or clear native electrophoresis (CNE) for separation of the mitochondrial complexes (19–21). We asked whether monomeric and dimeric/oligomeric ATP synthases differ with respect to their subunit compositions. Unlike the situation in yeast (22), subunits e and g are known as tightly bound subunits of monomeric bovine ATP synthase and therefore cannot be considered as dimer-specific subunits. However, no thorough search for other potential differences in the subunit composition of monomeric and dimeric or oligomeric ATP synthases has been performed so far.

The focus of the present work was to characterize the protein constituents of monomeric and dimeric mammalian ATP synthases by mass spectrometry and Edman protein sequencing to identify potential dimer-specific or ATP synthase-associated proteins. In a second step we planned to apply multidimensional electrophoresis, MS and tandem MS, and immunological techniques to verify or dismiss individual candidate proteins as dimer-specific or ATP synthase-associated proteins.

From the ‡Institut für Pharmazeutische Chemie, Biozentrum, Centre of Excellence "Macromolecular Complexes," Johann Wolfgang Goethe-Universität Frankfurt, Max-von-Laue-Str. 9, D-60439 Frankfurt am Main, Germany, §Molekulare Bioenergetik, Zentrum der Biologischen Chemie, Centre of Excellence "Macromolecular Complexes," Fachbereich Medizin, Johann Wolfgang Goethe-Universität Frankfurt, Theodor-Stern-Kai 7, D-60590 Frankfurt am Main, Germany, and ¶Chimie Organique des Substances Naturelles, CNRS, 5 Rue Blaise Pascal, 67084 Strasbourg Cedex, France

Received, March 6, 2007, and in revised form, June 6, 2007

Published, MCP Papers in Press, June 17, 2007, DOI 10.1074/mcp.M700097-MCP200

[1] The abbreviations used are: complex I, NADH dehydrogenase complex; complex III, ubiquinol cytochrome *c* reductase; complex IV, cytochrome *c* oxidase; complex V, ATP synthase; BN, blue native; CN, clear native; BNE, blue native electrophoresis; CNE, clear native electrophoresis; DDM, dodecylmaltoside; PMF, peptide mass fingerprint; DAPIT, diabetes-associated protein in insulin-sensitive tissue; 1-D, one-dimensional; 2-D, two-dimensional; dSDS, doubled SDS; Tricine, *N*-[2-hydroxy-1,1-bis(hydroxymethyl)ethyl]glycine; Su, subunit.

EXPERIMENTAL PROCEDURES

Materials—6-Aminohexanoic acid, imidazole, and digitonin (catalog number 37006, purity >50%) were obtained from Fluka. Digitonin was used directly without recrystallization. Acrylamide and bisacrylamide (the commercial 2× crystallized products), and Coomassie Blue G-250 (Serva Blue G) were purchased from Serva, bovine trypsin was from Roche Applied Science, and α-cyano-4-hydroxycinnamic acid was from Bruker Daltonics, Bremen, Germany. All other chemicals were from Sigma.

Isolation of Mitochondria—Rat heart mitochondria were prepared according to Jacobus and Saks (23) but without using bovine serum albumin and trypsin. Crude mitochondria were further purified on a sucrose step gradient as described for yeast mitochondria (24) except that the layers contained 15, 23, 32, 37, 47, 55, and 60% sucrose. The band on top of the 47% sucrose layer contained the purified mitochondria. Aliquots containing 400 μg of mitochondrial protein or multiples thereof were sedimented by 10-min centrifugation at 10,000 × *g* and stored at −80 °C. Crude bovine heart mitochondria were prepared according to Smith (25).

Sample Preparation for Blue Native Electrophoresis—Aliquots containing 400 μg of sedimented mitochondrial protein were solubilized by adding 40 μl of solubilization buffer (50 mM NaCl, 50 mM imidazole, 2 mM 6-aminohexanoic acid, 1 mM EDTA, pH 7) and specific detergent amounts to set the detergent/protein ratios given in the text, *e.g.* 4 μl of digitonin (20% stock in water) was added to set a digitonin/protein ratio of 2 (g/g). Following 15-min centrifugation at 100,000 × *g*, Coomassie dye (2 μl from a 5% Coomassie G-250 stock in 750 mM 6-aminohexanoic acid) was added to the supernatant for BNE to set a detergent/Coomassie ratio of 8:1. The total supernatants were applied to two 0.15 × 0.5-cm sample gel wells each for BNE.

Electrophoretic Techniques and Gels—Buffers and running conditions for 1-D BNE and 2-D BNE/BNE were as described previously (26). Linear 3–13% acrylamide gradient gels were used for 1-D BNE, and linear 4–16% acrylamide gradient gels were used for 2-D BNE (with 0.02% dodecylmaltoside added to the cathode buffer). SDS-PAGE was performed as described recently (27) using 16% T, 6% C gels, the optimal gel type for resolution of bovine ATP synthase subunits. Electroblotting onto PVDF membranes and doubled SDS-PAGE (dSDS-PAGE) followed recent protocols (27, 28).

Antibodies and Western Blotting—PVDF membranes were destained for 5 min in methanol and washed for 30 min in PBS, 0.5% Tween 20 and for 5 min in PBS, 0.1% Tween 20. Following a 16-h incubation with specific antibody diluted in PBS, 0.1% Tween 20, the membrane was washed three times for 10 min in PBS, 0.1% Tween 20. Blots were then incubated for 1 h with goat anti-rabbit immunoglobulin G conjugated to horseradish peroxidase (Sigma, catalog number A0545) diluted 1:20,000 by PBS, 0.1% Tween 20. Blots were washed five times for 5 min in water followed by a chemiluminescence assay.

A polyclonal rabbit antibody raised against the bovine MLQ protein (29) was used at 1:2500 dilution. Antisera against amino- and carboxyl-terminal sequence stretches of the AGP protein (AGPEADAQFHFTGIK and YFKLRSKKTPAVKAT) coupled to keyhole limpet hemocyanin via a cysteine residues were raised in rabbits (Eurogentec, Seraing, Belgium). 1:10,000–1:40,000 dilutions were used for immunodetection.

In-gel ATP Hydrolysis Assay and Densitometric Quantification—Phosphate that was produced by the in-gel ATP hydrolysis activity of complex V bands precipitated as white lead phosphate bands during the assay, and the white precipitates were quantified densitometrically. The assay followed the protocol of Zerbetto *et al.* (30) except that the 1-D BN gel was preincubated for 1 h in 35 mM Tris, 270 mM glycine buffer, pH 8.3, before this buffer was exchanged for the assay buffer containing 8 mM ATP, 0.2% lead nitrate, and 14 mM magnesium sulfate. The 1-h preincubation raised the sensitivity of the ATPase assay considerably approaching the high sensitivity of the assay using CN gels. In contrast to CN gels, however, the ATP hydrolysis activity could not be inhibited by the complex V inhibitor oligomycin (5 μg/ml added to preincubation and assay buffers). After 60 min the assay had to be stopped by 30-min incubation in 50% methanol and transfer to water. Documentation of the white precipitates by standard color scanning was optimal using black cover sheets. Chemi Doc XRS (Bio-Rad) and the Quantity One software (Bio-Rad) were used for densitometric quantification on native and SDS gels using non-condensed tiff files.

Following documentation, the lead phosphate precipitates were dissolved by 10% acetic acid, and the gel was restained by Coomassie dye to identify further mitochondrial complexes. Because bands in 1-D BNE were rarely useful for densitometric quantitation, representative subunits of complexes on Coomassie-stained 2-D SDS gels were used instead for more reliable quantification. Using the Coomassie-stained α and β subunits of complex V, for example, and the densitometric data for the in-gel lead phosphate precipitates, specific activities for the various oligomeric states of complex V were calculated.

Edman Degradation—Electroblotted proteins on PVDF membranes were sequenced directly using a 473A protein sequencer (Applied Biosystems) or after incubation in a 1:1 (v/v) mixture of trifluoroacetic acid and methanol (24 h at 37 °C for deformylation; 57 h at 37 °C for partial deacylation) (31). Internal protein sequences were obtained as described previously (32). Briefly complex V subunits were separated by blue SDS-PAGE. Individual subunits were extracted by electroelution and cleaved at tryptophan residues by *o*-iodosobenzoic acid in 80% acetic acid (33). Acetic acid was diluted with 9 volumes of water and then removed by lyophilization. Dried samples were redissolved by adding a minimal volume of water and 0.5% mercaptoethanol. Protein fragments were then separated by Tricine-SDS-PAGE and electroblotted on PVDF membranes for protein sequencing.

Sample Preparation for Mass Spectrometry—Silver-stained protein spots were destained with 100 μl of 15 mM potassium ferricyanide(III), 50 mM sodium thiosulfate; washed three times with H_2O (400 μl, 15 min) and three times with 50% (v/v) acetonitrile, 25 mM NH_4HCO_3 (400 μl, 15 min); and prepared for mass spectrometry essentially as described previously (34). Briefly following overnight trypsin digestion, the supernatant was collected. The gel pieces were then extracted twice for 30 min by 50% (v/v) acetonitrile, 5% (v/v) formic acid followed by two extractions for 30 min using 100% (v/v) acetonitrile, 5% (v/v) formic acid. The combined extracts were dried by SpeedVac and stored at −20 °C for mass spectrometric analysis.

MALDI-TOF and MALDI-TOF/TOF Mass Spectrometry—Dried samples were dissolved in 5 μl of 50% (v/v) acetonitrile, 0.5% (v/v) trifluoroacetic acid. 1 μl of sample was mixed with 1 μl of matrix (half-saturated α-cyano-4-hydroxycinnamic acid in 50% (v/v) acetonitrile, 0.5% (v/v) trifluoroacetic acid) and dried in ambient air. The crystals were washed briefly with ice-cold 5% (v/v) formic acid. MS experiments were performed on the Ultraflex TOF/TOF instrument (Bruker Daltonics). The low mass gate was set to 650 Da, and the acquisition range was set to 700–5000 Da. Approximately 1200 scans were accumulated for each mass spectrum. The obtained resolution was ~15,000 at $m/z = 2000$. Using external calibration mass accuracy was 50 ppm. A standard peptide calibration mixture (Applied Biosystems/MDS SCIEX) that contained six peptides covering the acquired mass range was used for the calibration (see Supplemental Table S6*A*). Selected peaks of ATP synthase subunits were fragmented by the LIFT method to verify peptide mass fingerprint identifications with a mass accuracy of 50 ppm for the precursor and 0.6 Da for the fragments. The isolation width for the precursor was adjusted manually (0.5–1% of the precursor mass), and the following

fragmentation was laser-induced using 2000–10,000 scans.

Analysis of Mass Spectrometric Data—All MS spectra were smoothed, noise-filtered, and monoisotopically labeled using Flex Analysis version 2.2 software (Bruker Daltonics). Monoisotopic peaks with a signal-to-noise ratio >3 were annotated using the Sophisticated Numerical Annotation Procedure (SNAP) algorithm (see Supplemental Table S6B). Peaks present in almost all MS spectra were defined as contaminants even if the peaks could not be classified as trypsin peaks, matrix clusters, or other laboratory-specific contaminants like keratin. These peaks were removed from the mass list prior to database search (background peak list, Supplemental Table S3). The generated peak lists were searched against the National Center for Biotechnology Information non-redundant (NCBInr) March 26, 2007 (4,761,919 sequence entries) database using Mascot search engine (version 2.2, Matrix Science Ltd., London, UK) (35). Searches were done with tryptic specificity allowing two missed cleavages. MS spectra from gel spots with masses below 15 kDa were checked allowing up to five missed cleavages (*e.g.* spot 15 in Supplemental Table S1 and Supplemental Fig. S22). Mass tolerance was set to 50 ppm. Carbamidomethylation of cysteine and oxidation of methionine were allowed structure modifications, and the Rodentia database subset was chosen (163,720 sequence entries). Mascot scores greater than 65 were considered significant. Additionally the Mascot score of the first non-homologous protein to the highest ranked hit was checked (see Supplemental Table S4). All PMF searches were also repeated against a randomized database (see Supplemental Table S5). Search results were finally transferred to BioTools version 2.2 software (Bruker Daltonics) for visualization (see Supplemental Table S1 and Supplemental Figs. S1–S22).

MS/MS spectra were processed and searched similarly except that the signal-to-noise threshold for the monoisotopic labeling was 6 and that the maximal number of allowed peaks was 50 (see Supplemental Table S6C). These strict settings for the peak labeling ensure a high quality of the mass lists submitted to the database search. Searches were done with individual MS/MS spectra using MALDI-TOF/TOF as instrument type and a 50-ppm mass tolerance for the precursor and a 0.6-Da mass tolerance for the fragments. Database, search engine, and search parameters were used as for the PMF search. A decoy database search was also carried out (see Supplemental Table S2). BioTools version 2.2 software (Bruker Daltonics) was used for visualization of the MS/MS database search results. The strict settings for the peak labeling were lowered before calculating the fragmentation patterns of the identified peptides (signal-to-noise threshold >1.5, maximal number of allowed peaks = 200; Supplemental Table S6C). Peptides were considered as identified when the scoring value exceeded the identity or extensive homology threshold value calculated by Mascot version 2.2 (threshold, 2; listed in Supplemental Table S2) or the significant homology value (threshold, 1; listed in Supplemental Table S2). Spectra with scores below or close to the significant homology value were manually inspected. Peptides were regarded as identified when prominent fragments of laser-induced dissociation (y, b, a, and immonium ions) could be assigned to the calculated fragmentation patterns (BioTools version 2.2 software, Bruker Daltonics) of the peptide (Supplemental Figs. S9, S11, and S17–S19).

Programs Used for Structural Analysis and Homologue Search—Analysis was done with freeware provided by the ExPASy Proteomics Server (Swiss Institute of Bioinformatics; www.expasy.org), NCBI (www.ncbi.nlm.nih.gov), and the *Saccharomyces* Genome Database (www.yeastgenome.org). The prediction of transmembrane regions was done with TMpred, SOSUI, TMHMM version 2.0, and HMMTOP version 2.2, and the search for putative phosphorylation sites was performed by NetPhos version 2.0 (www.expasy.org). blastp searches were done using NCBI database and *Saccharomyces* Genome Database, respectively (search date, March 2007; search settings summarized in Supplemental Table S7). ClustalW version 1.83 (www.expasy.org) was used for direct alignments of protein sequences.

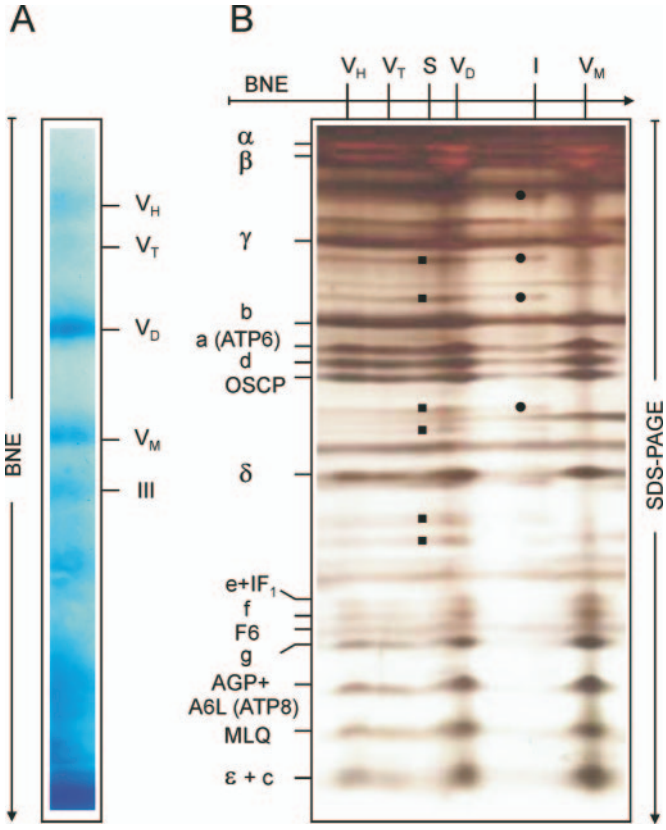

FIG. 1. **1-D and 2-D resolution of bovine ATP synthase for Edman degradation.** *A*, complex V or ATP synthase was solubilized as monomer (V_M), dimer (V_D), tetramer (V_T), and hexamer (V_H) from bovine heart mitochondria by digitonin (2 g/g of protein) and resolved by 1-D BNE. *III*, respiratory chain complex III. *B*, the 1-D BN gel strip was resolved by 2-D Tricine-SDS-PAGE using 16% T, 6% C acrylamide gels and silver-stained. Subunits were assigned according to the results of Edman degradation. Two novel proteins with amino-terminal sequences AGP and MLQ were identified in the columns of subunits for complex V monomer (V_M) and dimer (V_D). Minor amounts of subunits of complex I (*I*; ●) and of contaminating respiratory chain supercomplexes (*S*; ■) are marked.

RESULTS

Identification of Two Proteins Co-migrating with Bovine ATP Synthase in 1-D Blue Native Gels—Digitonin-solubilized ATP synthase from mammalian mitochondria is a mixture of oligomeric forms (20, 21). Using a low digitonin/protein ratio of 2 (g/g) for solubilization, BNE separated monomeric and dimeric ATP synthases as the predominant forms and significantly lower amounts of the tetrameric and hexameric forms as shown in Fig. 1. Respiratory complexes and supercomplexes could not be detected in 1-D BNE under these solubilization conditions with the exception of some respiratory complex III (Fig. 1*A*). Several subunits of complex I (*dots*) and of respiratory chain supercomplexes (*squares*) were identified as major contaminants of ATP synthase after 2-D resolution by SDS-PAGE (Fig. 1*B*).

Bands of monomeric and dimeric ATP synthases were then extracted from similar BN gels performed on a preparative scale. Following SDS-PAGE and electroblotting onto PVDF membranes the protein subunits were identified by Edman degradation. Direct amino-

terminal sequencing, sequencing of internal fragments of subunits d, f, and g cleaved at tryptophan (see "Experimental Procedures"), and sequencing of deformylated subunits a and A6L were used to identify and assign the well known subunits of ATP synthase as labeled in Fig. 1*B*. In addition to the sequences of known ATP synthase subunits, direct amino-terminal sequencing revealed sequence stretches MLQSLIKKVWIPMKPYYTQAYQEI and AGPEADAQFHFTGIKKYFN for two further proteins, the MLQ and AGP proteins, respectively (see Fig. 6). Database searches using these query sequences identified two proteins with known sequences. The MLQ protein had been described as 6.8-kDa mitochondrial proteolipid due to its extractability by chloroform/methanol from mitochondrial membranes (29). The AGP protein had been described as diabetes-associated protein in insulin-sensitive tissue (DAPIT; Ref. 36).

At that stage it was not possible to decide whether the MLQ and AGP proteins were contaminations or ATP synthase-associated proteins. However, it was possible to exclude MLQ and AGP proteins as dimer-specific proteins because both proteins were identified in the dimeric and in the monomeric bovine ATP synthases as well.

Protein Composition of Highly Pure Rat Heart ATP Synthase Isolated by 2-D BNE/BNE—Next we asked how we could improve the purity of the analyzed complexes without disturbing detergent-sensitive protein-protein interactions and losing associated proteins. The highest purity of multiprotein complexes is prerequisite to analyze the subunit composition by mass spectrometry, but even this purity does not guarantee that identified proteins are true subunits or associated proteins. On the other hand, multistep isolation protocols using common detergents can dissociate proteins that are associated with protein complexes in the membrane, and any chance to identify associated proteins and potential regulatory factors is lost. As a compromise, we therefore applied a special 2-D electrophoretic technique that used native conditions for both dimensions (2-D BNE/BNE) to isolate highly pure membrane protein complexes under very mild conditions as exemplified in Fig. 2, *A* and *B*. Digitonin was used to solubilize rat heart mitochondria for 1-D BNE under very mild conditions to preserve supramolecular assemblies of respiratory chain complexes I, III, and IV, and dimeric ATP synthase. The following 2-D BNE used the same buffers as 1-D BNE except that 0.02% dodecylmaltoside was added to the Coomassie dye-containing cathode buffer. Detergent and anionic Coomassie dye formed negatively charged micelles that dissociated supramolecular assemblies into the individual complexes during the 2-D BNE except some dimeric complex V (Fig. 2*B*, V_D). The mixed Coomassie/detergent micelles have the potential to partly or completely remove associated proteins from the complexes during 2-D BNE. However, if some percentage of the MLQ and AGP proteins was still bound to complex V, mass spectrometry should be able to detect these residual amounts.

Monomeric complex V from 1-D BNE that retained its monomeric state during transition to 2-D BNE (Fig. 2*B*, *boxed red*) and monomeric complex V that was dissociated from dimeric complex V (Fig. 2*B*, *boxed black*) were detected as Coomassie-stained spots during the native 2-D electrophoresis. These spots were then cut out for further resolution by dSDS-PAGE (28), *i.e.* two orthogonal SDS gels with strongly differing separation properties were applied for three-dimensional and four-dimensional resolution as exemplified in Fig. 2*C*. The individual spots were then analyzed by mass spectrometry as summarized briefly in Table I and with more detail in Supplemental Table S1. If the result of the peptide mass fingerprint search was below or close to the significance threshold (Mascot score, 65), the protein identity was verified by MS/MS experiments (Fig. 2*C*, spots 8 and 9, Supplemental Table S2, and Supplemental Figs. S9 and S11). Spots containing protein mixtures were also analyzed by MS/MS experiments (Fig. 2*C*, spots 10 and 14, and Supplemental Table S2). None of the PMF and MS/MS database searches matched the randomized sequences of the decoy database (see Supplemental Tables S2 and S5), and the Mascot score of the highest ranked non-homologous protein was always clearly below the significance threshold (see Supplemental Table S4). Furthermore the relative molecular masses of all identified proteins corresponded to their apparent masses on the doubled SDS-PAGE (see Fig. 2*C* and Supplemental Table S1).

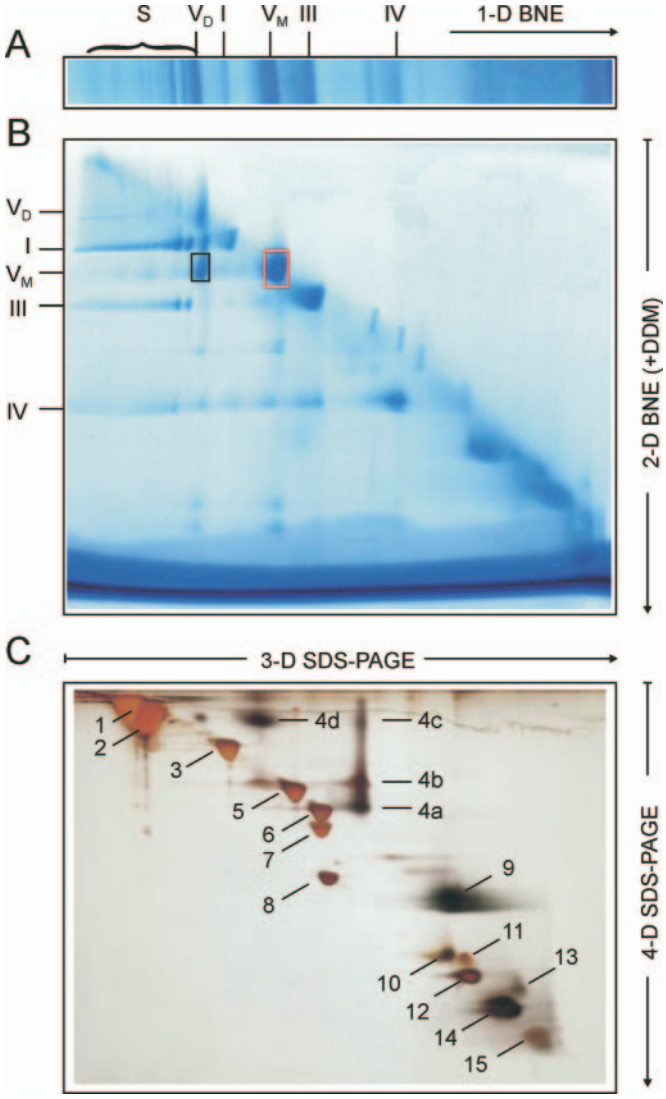

FIG. 2. **Multidimensional electrophoretic resolution of rat heart ATP synthase for mass spectrometric analyses.** *I*, *III*, and *IV*, respiratory chain complexes I, III, and IV, respectively; *S*, supercomplex associates of respiratory chain complexes I, III, and IV; V_D and V_M, dimeric and monomeric complex V, respectively. *A*, rat heart mitochondria were solubilized by digitonin (2 g/g of protein) and the mitochondrial complexes were resolved by 1-D BNE. *B*, a gel strip from 1-D BNE was resolved by 2-D BNE (+DDM) that used 0.02% dodecylmaltoside in the cathode buffer to dissociate supramolecular assemblies from the 1-D gel into the individual complexes. *C*, monomeric complex V (V_M; *boxed red* in *B*) was first resolved by three-dimensional Tricine-SDS-PAGE using 11% T, 3%C acrylamide, 6 M urea gels followed by four-dimensional Tricine-SDS-PAGE using 16% T, 6% C acrylamide gels. Assignment of subunits was according to mass spectrometric identification (Table I and supplemental data).

TABLE I

Mass spectrometrically identified proteins (except ATP6) from highly purified rat heart ATP synthase (Fig. 2C)

Number of transmembrane helices (TMH) as predicted by TMHMM (www.expasy.org). pI was calculated using BioTools version 2.2 (Bruker Daltonics). OSCP, oligomycin sensitivity conferral protein.

Spot no.	Su assignment	Accession no.	Protein mass	TMH	pI
			Da		
1	α	gi|6729934	55,361	0	8.9
2	β	gi|1374715	51,171	0	4.8
3	γ	gi|728931	30,229	0	9.4
4a–4d	ATP6 (or Su a)	gi|110189668	25,050	6	9.6
5	Su b	gi|19705465	28,965	0	9.9
6	OSCP	gi|20302061	23,440	0	10.5
7	Su d	gi|9506411	18,809	0	6.2
8	δ	gi|20806153	17,584	0	5.0
9	Su c	gi|8392939	14,235	2	11.4
10	F6	gi|16758388	12,487	0	9.9
	Su f	gi|109495163	10,503	1	10.5
11	Su e	gi|17978459	8,249	0	9.5
12	Su g	gi|47058994	11,453	0	9.9
13	AGP (or DAPIT)	gi|19424210	6,460	1	10.4
14	ATP8 (or A6L)	gi|110189667	7,637	1	9.8
	MLQ (or 6.8-kDa proteolipid)	gi|109478763	6,910	1	10.4
15	ϵ	gi|258789	5,689	0	10.6

Protein spots 4a–4d could not be identified. We assume that these four spots represent different conformations and aggregation states of subunit a or ATP6, which is the most hydrophobic subunit of ATP synthase. This assumption is supported by some common features of highly hydrophobic proteins: by the low number of tryptic fragments of appropriate size (see Supplemental Fig. S4), by the location in dSDS gels above the diagonal of common proteins with normal hydrophobicity, and by the rapid and strong silver staining (28). Spot 13, the AGP protein (36), was identified by peptide mass fingerprinting (Fig. 3*A*). Three MS/MS experiments verified the peak assignment (Supplemental Figs. S17–S19). The high number of basic amino acids at the carboxyl terminus of the AGP protein can explain the lack of tryptic fragments in the MS spectrum for this protein region. A large hydrophobic peptide (residues 28–46) comprising the central cluster of hydrophobic amino acids was generated. Several analysis programs predict a transmembrane helix in this region of the AGP protein. Extraction problems and suppression effects in the MALDI process can therefore explain the absence of a corresponding peak in the MS spectrum. The MLQ protein was found as a component of spot 14 together with subunit ATP8 (Supplemental Figs. S20 and S21). Three peaks matched the MLQ sequence. One signal was identified as the carboxyl-terminal part by MS/MS (Fig. 3*B*). Two further peaks could be assigned to short amino-terminal sequences. Similar to AGP, the carboxyl terminus of the MLQ protein was rich in basic amino acids. Therefore, trypsin could produce only one theoretical peptide with sufficient length for MS. Proline at sequence position 15 was predicted to generate a non-cleavable site and, together with a predicted transmembrane helix, to create a lipophilic peptide (residues 9–37). This peptide was not found in the MS spectrum presumably because it was not extractable from the gel.

Verification of MLQ and AGP as ATP Synthase-associated Proteins—Following identification of the MLQ and AGP proteins in bovine and rat ATP synthase preparations, we tried to verify or dismiss these proteins as ATP synthase-associated proteins. A polyclonal antibody against isolated bovine MLQ protein (29) and an amino-terminal peptide antibody against the bovine AGP protein were used on 2-D blots (2-D BNE/SDS-PAGE). Using digitonin for 1-D BNE of bovine mitochondria, the antibodies detected the MLQ and AGP proteins only within the columns of subunits for the various ATP synthase forms (Fig. 4*A*, V_M–V_H).

Using low dodecylmaltoside/protein ratios (0.6 g/g) for 1-D BNE, both antibodies gave rise to signals within the columns of subunits for monomeric and dimeric ATP synthases, but some broad signal intensity extended to the running front of the 2-D gel (*right side*) especially for the MLQ protein (Fig. 4*B*, *lowest panel*). This indicated that major amounts of the AGP protein were still bound to ATP synthase under low dodecylmaltoside conditions, whereas the MLQ protein was more detergent-sensitive and more prone to dissociation. Using higher dodecylmaltoside/protein ratios (1.6 g/g), as commonly used for membrane protein isolations, changed the situation completely. Both proteins were almost fully dissociated from ATP synthase (Fig. 4*C*). ATP synthase-associated and also individual MLQ and AGP proteins were identified using Triton X-100 for solubilization (Fig. 4*D*). The MLQ and AGP proteins migrate to the anode in BNE despite their isoelectric points that are around 10 for both proteins because both proteins bind Coomassie dye. However, such rather basic proteins usually show considerable streaking as was also observed here.

Regarding specifically the result obtained with digitonin solubilization we conclude that the MLQ and AGP proteins bind almost quantitatively to the ATP synthase in the mitochondrial membrane. No significant amounts of the individual proteins, not associated with complexes, seem to exist in the membrane because almost no signal intensity was detected on the *right side* of the 2-D gels (Fig. 4*A*), whereas dissociated individual MLQ and AGP proteins were clearly identified in the control 2-D gels (Fig. 4, *B–D*). Binding of MLQ and AGP proteins was not restricted to the dimeric and/or higher oligomeric forms of ATP synthase but occurred also with the monomeric form (Fig. 4, *A*, *B*, and *D*).

MLQ and AGP Proteins Do Not Affect the ATP Hydrolysis Activity of Complex V—Bovine heart mitochondrial supercomplexes and individual complexes were solubilized using various digitonin/protein and dodecylmaltoside (DDM)/protein ratios and then separated by BNE (Fig. 5). The solubilization conditions were chosen to keep the AGP and MLQ proteins either quantitatively associated with complex V (digitonin/protein ratio = 2–4 g/g), to partly dissociate the MLQ protein from complex V (DDM/protein ratio = 0.6 g/g), or to remove both

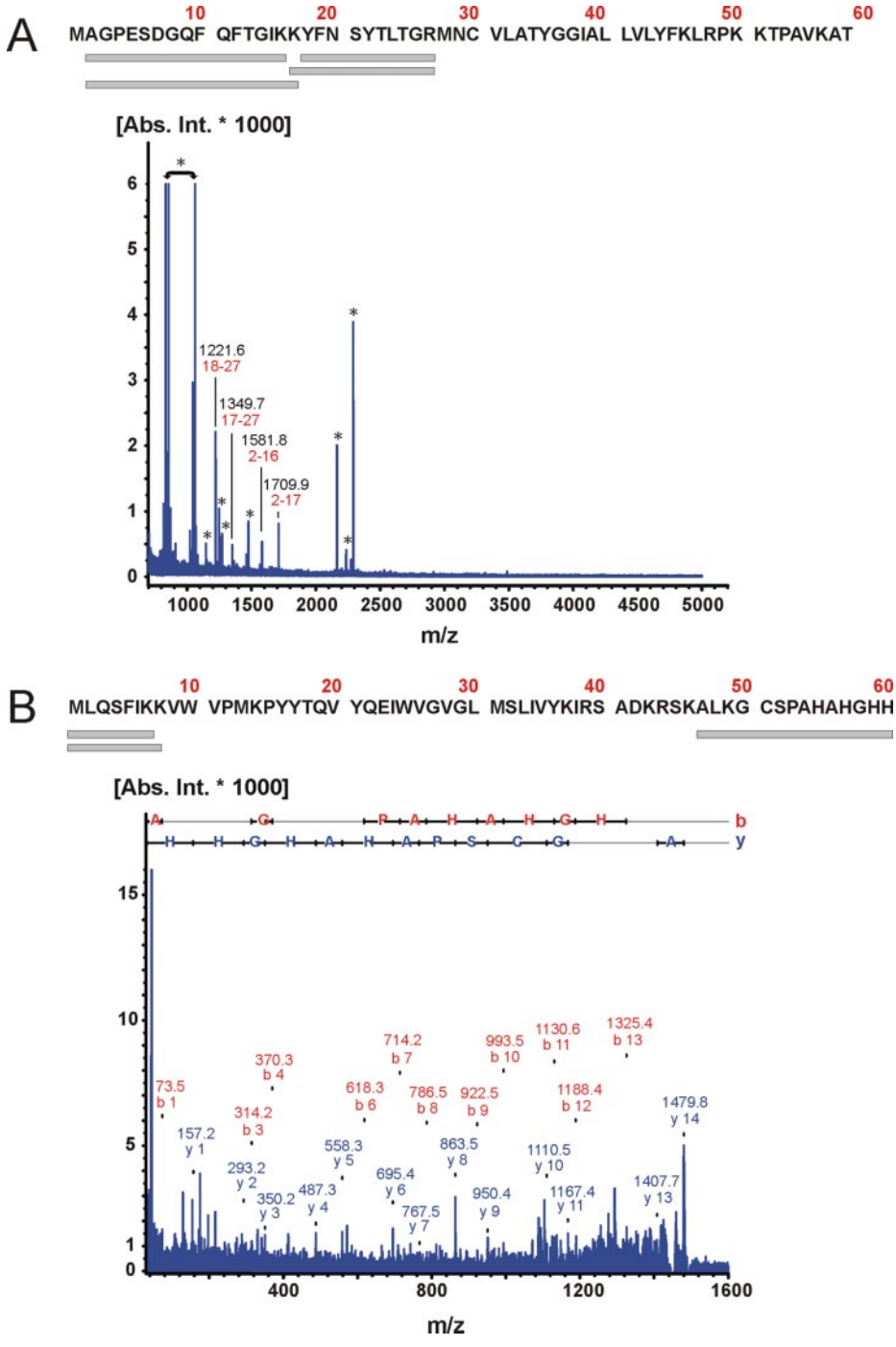

FIG. 3. **Mass spectrometric analysis of the AGP and MLQ proteins.** *A*, MS spectrum of the tryptic digest of the AGP protein (spot 13 in Fig. 2*C*). Masses were assigned to the AGP protein peaks. *Asterisks* mark background peaks. The bar plot aligns identified PMF fragments to the corresponding protein sequence regions (see also Supplemental Figs. S17–S19). *B*, MS/MS spectrum of the carboxyl-terminal tryptic fragment ALKGCSPAHAHGHH of the MLQ protein (spot 14 in Fig. 2*C*). For clarity, only fragments identified as b and y ions are indicated in the spectrum. The bar plot aligns the PMF fragments to the MLQ protein sequence (see also Supplemental Table S1 and Supplemental Figs. S20 and S21). Abs. Int., absolute intensity.

complex V-associated proteins almost completely (DDM/protein ratio = 1.6 g/g). The in-gel ATP hydrolysis activities (Fig. 5*A*) were then compared with the corresponding complex V protein amounts from densitometric quantitation of Coomassie-stained 2-D gels (not shown) to determine the specific ATP hydrolysis activities in the presence or absence of the novel complex V-associated proteins. As summarized in Table II, the specific ATP hydrolysis activity of monomeric complex V solubilized by high and low DDM amounts were almost identical, indicating that dissociation of the MLQ protein had no immediate effect on the catalytic activity of complex V. Also the specific ATP hydrolysis activities of monomeric complex V solubilized by DDM and digitonin were almost identical. This was not expected because different detergents in principle can delipidate proteins differentially and thereby influence catalytic activities.

Structural Analysis of the AGP and MLQ Proteins—Both proteins contain one putative transmembrane region (Fig. 6, *A* and *C*, marked *red*). Depending on the software used (www.expasy.org; TMPred, SOSUI, TMHMM, and HMMTOP) the position of the predicted helix varied marginally. A NetPhos search for phosphorylation sites (www.expasy.org) identified two possible phosphorylation sites (marked *blue*) for the AGP protein and one for the MLQ protein.

Search for AGP and MLQ Homologues—A protein-protein blast

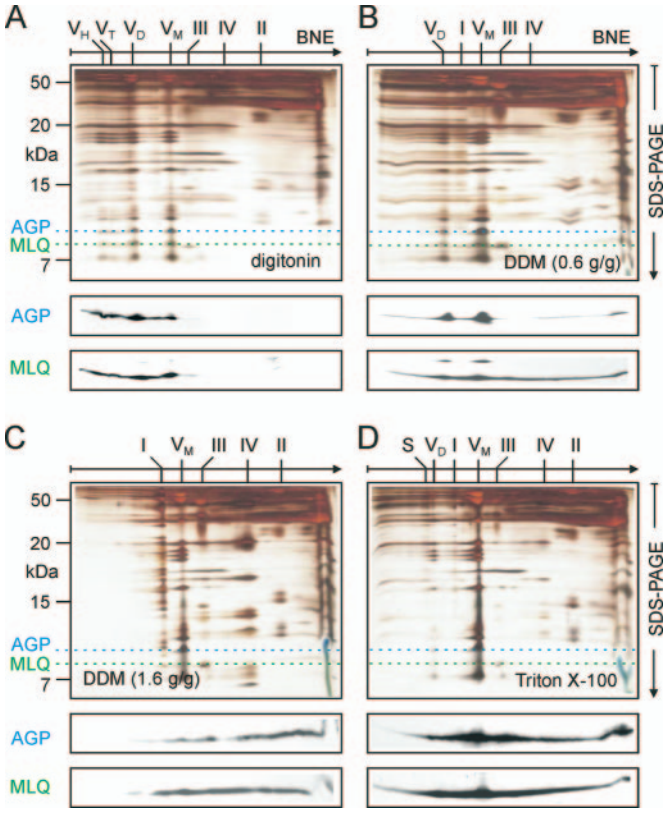

FIG. 4. **Verification of bovine MLQ and AGP proteins as ATP synthase-associated proteins.** Bovine heart mitochondria were solubilized by different detergents for 1-D BNE followed by 2-D Tricine-SDS-PAGE using 16% T, 6% C acrylamide gels. The detergent/protein ratios for 1-D BNE were: *A*, digitonin, 2 g/g; *B*, dodecylmaltoside, 0.6 g/g; *C*, dodecylmaltoside, 1.6 g/g; *D*, Triton X-100, 2.4 g/g. The 2-D gels were electroblotted onto PVDF membranes and analyzed using anti-MLQ and -AGP antibodies (*lower panels*). The expected location of the MLQ and AGP proteins in the 2-D gels is also indicated by *dotted lines*. *I*, *II*, *III*, and *IV*, respiratory chain complexes I, II, III, and IV, respectively; *S*, supercomplex associate of complexes I, III, and IV; V_M, V_D, V_T, and V_H, monomeric, dimeric, tetrameric, and hexameric complex V or ATP synthase, respectively.

search (blastp) using the *Rattus norvegicus* AGP protein sequence as query sequence to search the NCBI database identified mammalian proteins with around 90% identity and some insect orthologues (40% identity and 60% similarity comparing *R. norvegicus* and *Sarcophaga bullata* in Fig. 6*A*). A WU-BLAST2 search using the AGP homologous protein sequence of the insect *S. bullata* as query sequence to search the *Saccharomyces cerevisiae* genome database (www.yeastgenome.org) gave yeast ATP synthase subunit k at position six of the result list. However, sequence similarity between *S. bullata* AGP protein and *S. cerevisiae* subunit k was low (13% identity, 16% similarity), and the position of the predicted transmembrane helix was shifted (Fig. 6*B*). Similarly the rat AGP protein and yeast subunit k shared only 12% identical and 19% similar residues.

A homology search using the *R. norvegicus* MLQ protein sequence as query sequence to search the NCBI database identified several highly homologous mammalian proteins and one homologue (34% identity, 50% similarity) from the zebrafish *Danio rerio* (Fig. 6*C*). No homologue of the mammalian MLQ protein was found in the *S. cerevisiae* genome database. Direct comparison of MLQ with the known subunits of yeast ATP synthase did not reveal any similarity.

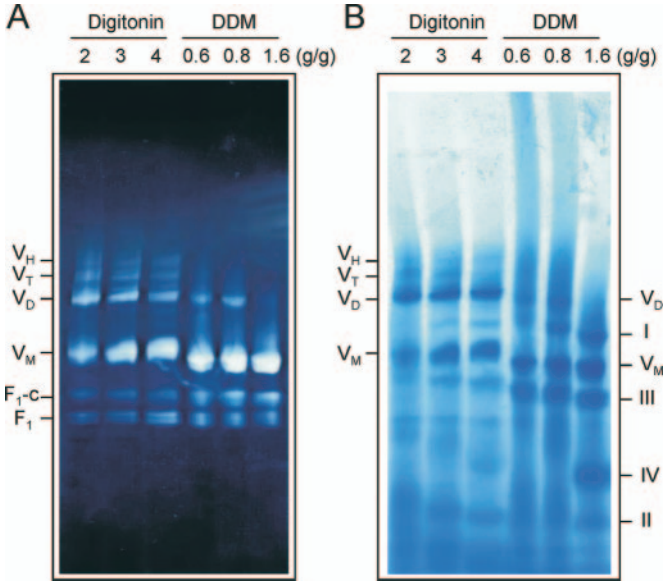

FIG. 5. **In-gel ATP hydrolysis activity of bovine ATP synthase bands containing or missing MLQ and AGP proteins.** Bovine heart mitochondria were solubilized using various digitonin/protein and DDM/protein ratios (2, 3, and 4 and 0.6, 0.8, and 1.6 g/g, respectively) and then separated by BNE. *A*, in-gel ATP hydrolysis/lead phosphate precipitation assay revealing bands of monomeric (V_M), dimeric (V_D), tetrameric (V_T), and hexameric (V_H) complex V. A doublet of low mass bands (F_1) represents F_1-subcomplexes containing and not containing bound inhibitor protein IF_1 according to previous analyses (38). A further band (F_1-c) located above contains a ring of c subunits in addition. MLQ and AGP proteins are missing in monomeric complex V using 1.6 g of DDM/g of protein. In contrast, both proteins are bound to all complex V bands under all digitonin solubilization conditions. *B*, the gel in *A* was restained by Coomassie as described under "Experimental Procedures." Respiratory complexes I–IV (*I–IV*) and monomeric (V_M) and dimeric (V_D) complex V are assigned.

DISCUSSION

Identification of complex-associated proteins is straightforward whenever mild purification protocols lead to co-isolation of known complexes and novel proteins as shown here. Subsequent verification of novel proteins as truly complex-associated proteins is facilitated if antibodies against the novel proteins and a high resolution separation technique like BNE are available. Exact or not exact co-localization of complex and novel proteins can verify or dismiss the novel proteins as complex-associated proteins. However, only permanently bound proteins can be identified by this approach. Identification of dynamic protein-protein interactions would require chemical cross-linking in the native environment prior to protein separation and proteomics analyses, which was not attempted here.

Mass spectrometric identification of proteins smaller than 10 kDa can pose a problem because the number of tryptic fragments of small proteins often is too low for successful database search and reliable identification. Furthermore small proteins often are not annotated as proteins in databases. For this work, however, searching nucleotide databases was not necessary because the two novel proteins were already an-

TABLE II

Invariable, MLQ- and AGP-independent, specific ATP hydrolysis activity of various oligomeric forms of complex V

As a measure for the specific ATP hydrolysis activity, the ratio of activity stain in 1-D BN gels and protein stain in 2-D SDS gels is given. +++ and + mark complexes containing high or reduced amounts, respectively, of bound MLQ or AGP proteins. — indicates almost complete loss of MLQ and AGP proteins.

	Detergent	Detergent/protein	Presence of MLQ	Presence of AGP	Specific ATPase activity
		g/g			
Monomeric complex V	DDM	0.6	+	+++	0.36 ± 0.05
		0.8	+	+++	0.26 ± 0.03
		1.6	—	—	0.28 ± 0.06
Monomeric complex V	Digitonin	2	+++	+++	0.34 ± 0.01
		3	+++	+++	0.32 ± 0.02
		4	+++	+++	0.30 ± 0.04
Dimeric complex V	Digitonin	2	+++	+++	0.27 ± 0.08
		3	+++	+++	0.32 ± 0.06
		4	+++	+++	0.29 ± 0.06
Tetrameric complex V	Digitonin	2	+++	+++	0.35 ± 0.08

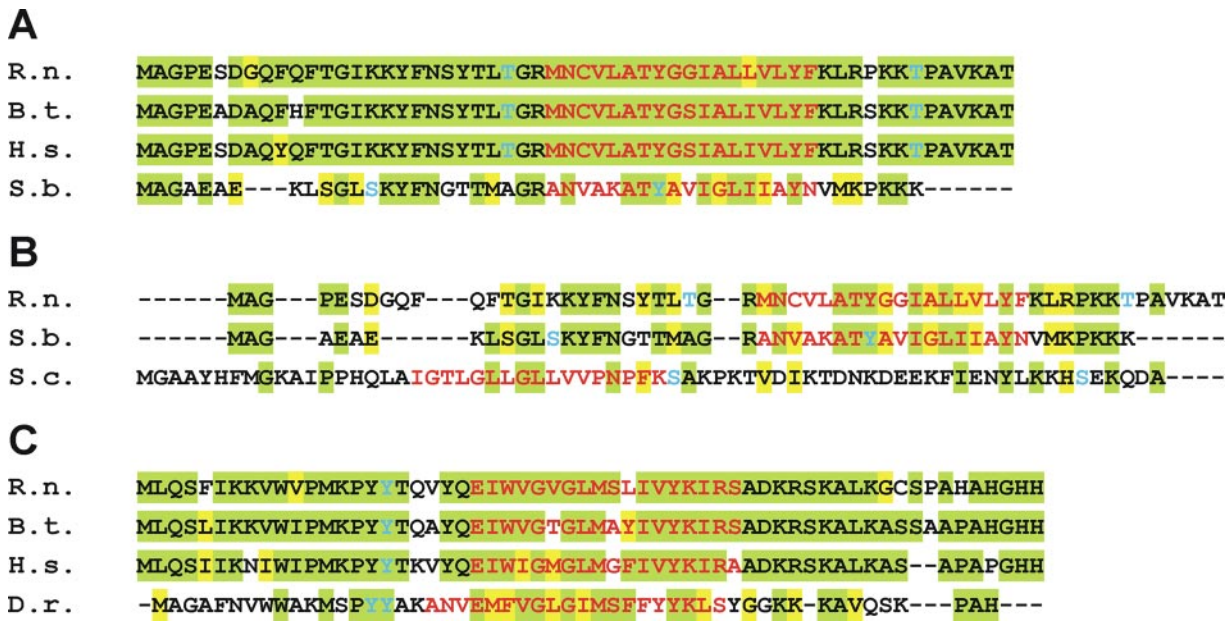

FIG. 6. **Alignment and structural analysis of the MLQ and AGP proteins.** Sequences were aligned using ClustalW (www.ebi.ac.uk). Transmembrane helices (marked *red*) were predicted by TMPred (www.expasy.org), phosphorylation sites (marked *blue*) were predicted by NetPhos (www.expasy.org). *Green*, *yellow*, and *unmarked* amino acids indicate identical, similar, and non-similar amino acids, respectively. *A*, alignment of AGP protein sequences from *R. norvegicus* (*R.n.*) (gi|19424210), *Bos taurus* (*B.t.*) (gi|91207977), *Homo sapiens* (*H.s.*) (gi|14249376), and *S. bullata* (*S.b.*) (gi|23505740). *B*, alignment of the AGP protein sequences from *R. norvegicus* (*R.n.*) and *S. bullata* (*S.b.*) and the ATP synthase subunit k from *S. cerevisiae* (*S.c.*) (gi|6324495). *C*, alignment of the MLQ protein sequences from *R. norvegicus* (*R.n.*) (gi|109478763), *B. taurus* (*B.t.*) (gi|112834), *H. sapiens* (*H.s.*) (gi|4758940), and *D. rerio* (*D.r.*) (gi 68394446).

notated in the NCBI database. Using highly purified complexes reduced potential ambiguities in the interpretation of the experimental data considerably. The AGP protein could be identified directly by peptide mass fingerprinting because it was detected as a distinct protein spot (Fig. 2*C*, spot 13) on a doubled SDS gel. MS/MS was then used for confirmation. The MLQ protein co-migrated with subunit 8 of ATP synthase (also named ATP8 or A6L subunit) and could not be identified by direct peptide mass fingerprinting. MS/MS analyses were required to identify this protein unambiguously in a mixture of proteins. This MLQ protein may well have escaped detection if the protein had not been identified before by Edman degradation using much larger amounts of relatively impure ATP synthase. We think that the power of Edman degradation should not be disregarded in times that are more and more reliant on ESI and MALDI MS techniques.

A NetPhos search for phosphorylation sites identified two potential phosphorylation sites for the AGP protein and one for the MLQ protein. This prediction was not confirmed by a recent proteomics study to search for posttranslational modifications of hydrophobic mitochondrial proteins (37). According to this careful study, the AGP or DAPIT protein (36) and the

MLQ protein (or 6.8-kDa proteolipid; Ref. 29) carry no post-translational modification. Reversible metabolic phosphorylation cannot be excluded.

Thorough subunit analyses are available for monomeric but not for dimeric ATP synthases except for dimeric ATP synthase from *S. cerevisiae* that contains three dimer-specific subunits, e, g, and k. The mammalian subunit e and g homologues are known as tightly bound subunits of monomeric bovine ATP synthase. Therefore, only the remaining yeast subunit k had to be analyzed for a potential similarity with the novel mammalian ATP synthase-associated proteins. A WU-BLAST2 search of the yeast genome database using an insect AGP query sequence revealed subunit k as a potential AGP homologue. However, the sequence similarity was low (13% identity, 16% similarity), and the position of the predicted transmembrane helix was shifted compared with the AGP protein. This suggested that the low similarity between the AGP protein and yeast ATP synthase subunit k might be fortuitous. Homology of AGP and subunit (Su) k proteins would not help much to elucidate the functional role of the mammalian AGP protein because deletion of Su k did not alter the yeast phenotype (22).

Alternative names for the AGP protein that might also give some hints for potential functional roles are usmg5 protein (up-regulated during skeletal muscle growth protein 5) and diabetes-associated protein in insulin-sensitive tissue. Up-regulation in response to active stretching of skeletal muscle and down-regulation of DAPIT mRNA in insulin-sensitive rat tissues upon induction of streptozotocin-induced diabetes may point to a role in the energy metabolism of cells, in glucose metabolism, and/or in oxidative phosphorylation. RNA silencing will be used to study possible AGP- and/or MLQ-dependent changes in the mitochondrial inner membrane morphology and in the supramolecular organization of oxidative phosphorylation complexes especially of the oligomeric state of the mitochondrial ATP synthase.

* This work was supported by the Deutsche Forschungsgemeinschaft, Sonderforschungsbereich 472 Project P11 (to H. S.) and Sonderforschungsbereich 628 Project P13 (to M. K. and H. S.). The costs of publication of this article were defrayed in part by the payment of page charges. This article must therefore be hereby marked "*advertisement*" in accordance with 18 U.S.C. Section 1734 solely to indicate this fact.

S The on-line version of this article (available at http://www.mcponline.org) contains supplemental material.

‖ To whom correspondence should be addressed: Molekulare Bioenergetik, Zentrum der Biologischen Chemie, Fachbereich Medizin, Universität Frankfurt, Theodor-Stern-Kai 7, Haus 26, D-60590 Frankfurt am Main, Germany. Tel.: 49-69-6301-6927; Fax: 49-69-6301-6970; E-mail: schagger@zbc.kgu.de.

REFERENCES

1. Hatefi, Y. (1985) The mitochondrial electron transport and oxidative phosphorylation system. *Annu. Rev. Biochem.* **54,** 1015–1069
2. Saraste, M. (1999) Oxidative phosphorylation at the fin de siècle. *Science* **283,** 1488–1493
3. Boyer, P. D. (1999) The ATP synthase—a splendid molecular machine. *Annu. Rev. Biochem.* **66,** 717–749
4. Abrahams, J. P., Leslie, A. G., Lutter, R., and Walker, J. E. (1994) Structure at 2.8 Å resolution of F_1-ATPase from bovine heart mitochondria. *Nature* **370,** 621–628
5. Gibbons, C., Montgomery, M. G., Leslie, A. G., and Walker, J. E. (2000) The structure of the central stalk in bovine F_1-ATPase at 2.4 Å resolution. *Nat. Struct. Biol.* **11,** 1055–1061
6. Karrasch, S., and Walker, J. E. (1999) Novel features in the structure of bovine ATP synthase. *J. Mol. Biol.* **290,** 379–384
7. Rubinstein, J. L., Walker, J. E., and Henderson, R. (2003) Structure of the mitochondrial ATP synthase by electron microscopy. *EMBO J.* **22,** 6182–6192
8. Rubinstein, J. L., Dickson, V. K., Runswick, M. J., and Walker, J. E. (2005) ATP synthase from *Saccharomyces cerevisiae*: location of subunit h in the peripheral stalk region. *J. Mol. Biol.* **345,** 513–520
9. Cabezon, E., Montgomery, M. G., Leslie, A. G., and Walker, J. E. (2003) The structure of bovine F_1-ATPase in complex with its regulatory protein IF_1. *Nat. Struct. Biol.* **10,** 744–750
10. Sabbert, D., Engelbrecht, S., and Junge, W. (1996) Intersubunit rotation in active F-ATPase. *Nature* **381,** 623–625
11. Noji, H., Yasuda, R., Yoshida, M., and Kinosita, K. (1997) Direct observation of the rotation of F_1-ATPase. *Nature* **386,** 299–302
12. Stock, D., Leslie, A. G., and Walker, J. E. (1999) Molecular architecture of the rotary motor in ATP synthase. *Science* **286,** 1700–1705
13. Seelert, H., Poetsch, A., Dencher, N. A., Engel, A., Stahlberg, H., and Muller, D. J. (2000) Structural biology. Proton-powered turbine of a plant motor. *Nature* **405,** 418–419
14. Collinson, I. R., Runswick, M. J., Buchanan, S. K., Fearnley, I. M., Skehel, J. M., van Raaij, M. J., Griffiths, D. E., and Walker, J. E. (1994) Fo membrane domain of ATP synthase from bovine heart mitochondria: purification, subunit composition, and reconstitution with F_1-ATPase. *Biochemistry* **33,** 7971–7978
15. Pullman, M. E., and Monroy, G. C. (1963) A naturally occurring inhibitor of mitochondrial adenosine triphosphatase. *J. Biol. Chem.* **238,** 3762–3769
16. Schwerzmann, K., and Pedersen, P. L. (1986) Regulation of the mitochondrial ATP synthase/ATPase complex. *Arch. Biochem. Biophys.* **250,** 1–18
17. Cabezon, E., Arechaga, I., Jonathan, P., Butler, G., and Walker, J. E. (2000) Dimerization of bovine F_1-ATPase by binding the inhibitor protein, IF_1. *J. Biol. Chem.* **275,** 28353–28355
18. Cabezon, E., Butler, P. J., Runswick, M. J., and Walker, J. E. (2000) Modulation of the oligomerization state of the bovine F_1-ATPase inhibitor protein, IF_1, by pH. *J. Biol. Chem.* **275,** 25460–25464
19. Schägger, H., and Pfeiffer, K. (2000) Supercomplexes in the respiratory chains of yeast and mammalian mitochondria. *EMBO J.* **19,** 1777–1783
20. Krause, F., Reifschneider, N. H., Goto, S., and Dencher, N. A. (2005) Active oligomeric ATP synthases in mammalian mitochondria. *Biochem. Biophys. Res. Commun.* **329,** 583–590
21. Wittig, I., and Schägger, H. (2005) Advantages and limitations of clear native polyacrylamide gel electrophoresis. *Proteomics* **5**, 4338–4346
22. Arnold, I., Pfeiffer, K., Neupert, W., Stuart, R. A., and Schägger, H. (1998) Yeast mitochondrial F_1F_0-ATP synthase exists as a dimer: identification of three dimer-specific subunits. *EMBO J.* **17,** 7170–7178
23. Jacobus, W. E., and Saks, V. A. (1982) Creatine kinase of heart mitochondria: changes in its kinetic properties induced by coupling to oxidative phosphorylation. *Arch. Biochem. Biophys.* **219,** 167–178
24. Meisinger, C., Sommer, T., and Pfanner, N. (2000) Purification of *Saccharomyces cerevisiae* mitochondria devoid of microsomal and cytosolic contaminations. *Anal. Biochem.* **287,** 339–342
25. Smith, A. L. (1967) Preparation, properties, and conditions for assay of mitochondria: slaughterhouse material, small-scale. *Methods Enzymol.* **10,** 81–86
26. Wittig, I., Braun, H. P., and Schägger, H. (2006) Blue-native PAGE. *Nat. Protoc.* **1,** 416–428
27. Schägger, H. (2006) Tricine-SDS-PAGE. *Nat. Protoc.* **1,** 16–22
28. Rais, I., Karas, M., and Schägger, H. (2004) Two-dimensional electrophoresis for the isolation of integral membrane proteins and mass spectrometric identification. *Proteomics* **4,** 2567–2571
29. Terzi, E., Boyot, P., Van Dorsselaer, A., Luu, B., and Trifilieff, E. (1990) Isolation and amino acid sequence of a novel 6.8-kDa mitochondrial proteolipid from beef heart. Use of FAB-MS for molecular mass deter-

mination. *FEBS Lett.* **260,** 122–126
30. Zerbetto, E., Vergani, L., and Dabbeni-Sala, F. (1997) Quantification of muscle mitochondrial oxidative phosphorylation enzymes via histochemical staining of blue native polyacrylamide gels. *Electrophoresis* **18,** 2059–2064
31. Gheorghe, M. T., Jornvall, H., and Bergman, T. (1997) Optimized alcoholytic deacetylation of N-acetyl blocked polypeptides for subsequent Edman degradation. *Anal. Biochem.* **254,** 119–125
32. Hunte, C., von Jagow, G., and Schägger, H. (2003) *Membrane Protein Purification and Crystallization*, 2nd Ed., pp. 97–103, Academic Press, San Diego, CA
33. Mahoney, W. C., Smith, P. K., and Hermodson, M. A. (1981) Fragmentation of proteins with o-iodosobenzoic acid: chemical mechanism and identification of o-iodoxybenzoic acid as a reactive contaminant that modifies tyrosyl residues. *Biochemistry* **20,** 443–448
34. Shevchenko, A., Wilm, M., Vorm, O., and Mann, M. (1996) Mass spectrometric sequencing of proteins on silver-stained polyacrylamide gels. *Anal. Chem.* **68,** 850–858
35. Perkins, D. N., Pappin, D. J., Creasy, D. M., and Cottrell, J. S. (1999) Probability-based protein identification by searching sequence databases using mass spectrometry data. *Electrophoresis* **20,** 3551–3567
36. Paivarinne, H., and Kainulainen, H. (2001) DAPIT, a novel protein downregulated in insulin-sensitive tissues in streptozotocin-induced diabetes. *Acta Diabetol.* **38,** 83–86
37. Carroll, J., Fearnley, I. M., and Walker, J. E. (2006) Definition of the mitochondrial proteome by measurement of molecular masses of membrane proteins. *Proc. Natl. Acad. Sci. U. S. A.* **103,** 16170–16175
38. Wittig, I., Carrozzo, R., Santorelli, F. M., and Schagger, H. (2006) Supercomplexes and subcomplexes of mitochondrial oxidative phosphorylation. *Biochim. Biophys. Acta* **1757,** 1066–1072